

when  $\omega$  is small,<sup>1</sup> which dependence may be inferred from the experiments on Tb-Y, Tb-Lu, and Tb-Sc<sup>16</sup> alloys as well as for the rare-earth elements. It is also consistent with the fact<sup>1</sup> that when as little as 10% La, which generally tends to diminish  $\omega$ , is added to Tb, the helical structure becomes unstable and the ferromagnetic structure ( $\omega=0$ ) is realized. The microscopic explanation for this is not clear as yet.

<sup>16</sup> H. R. Child and W. C. Koehler, *J. Appl. Phys.* **37**, 1353 (1966).

## ACKNOWLEDGMENTS

The authors would like to thank V. J. Minkiewicz and J. Skalyo for valuable discussions and F. Langdon for technical assistance in the high-pressure equipment. They also wish to express their gratitude to Professor F. H. Spedding and his colleagues at Ames Laboratory and to Dr. R. J. Gambino of IBM Watson Research Center, who kindly provided crystals used in this experiment.

## Heat Capacity of $\text{Mn}(\text{NH}_4)_2(\text{SO}_4)_2 \cdot 6\text{H}_2\text{O}$ near Its Critical Point\*

MARTIN RAYL,<sup>†</sup> O. E. VILCHES,<sup>‡</sup> AND J. C. WHEATLEY<sup>‡</sup>

*Department of Physics and Materials Research Laboratory, University of Illinois, Urbana, Illinois*

(Received 7 August 1967)

Measurements of the heat capacity of manganese ammonium Tutton salt as close as  $4.8 \times 10^{-5}$  °K to  $T_c$  ( $\approx 0.176$ °K) are presented. The measurements were made using both a cerium magnesium nitrate and a chromium potassium alum thermometer. Power- and logarithmic-law fits to the data are possible above  $\epsilon \approx 10^{-3}$  for a limited range of  $\epsilon = (T - T_c)/T_c$ . In the power-law fit the heat capacity varies as  $\epsilon^{-1/8}$ . For smaller  $\epsilon$ , a pronounced rounding of the heat capacity is observed below and above  $T_c$ . In every series of measurements, a  $T_c$  could be defined with an accuracy in  $\epsilon$  better than  $3 \times 10^{-5}$ . A comparison with measurements on other magnetic transitions and a simple hypothesis to explain the "rounding" of the peak are also presented.

### I. INTRODUCTION

RECENTLY there has been a great increase<sup>1-7</sup> in theoretical and experimental interest in static phenomena in the vicinity of critical points. The temperature dependence of the heat capacity very near the critical point is one of the quantities of primary interest in this field. The expected temperature dependence can be described by

$$\begin{aligned} C_+ &= A_+ \epsilon^{-\alpha} + B_+, \\ C_- &= A_- |\epsilon|^{-\alpha'} + B_-, \end{aligned} \quad (1)$$

\* This work has been supported by the U.S. Atomic Energy Commission at the University of Illinois under Contract No. AT(11-1)-1198 and in part at the University of California at San Diego under Contract No. AT(11-1)-34 P.A. 143.

<sup>†</sup> Present address: R. C. A. Laboratories, David Sarnoff Research Center, Princeton, N.J.

<sup>‡</sup> Present address: Department of Physics, University of California at San Diego, La Jolla, Calif. 92037.

<sup>1</sup> M. E. Fisher, in *Lectures in Theoretical Physics* (University of Colorado Press, Boulder, Colo., 1965), Vol. 7c, p. 1.

<sup>2</sup> M. E. Fisher, *J. Math. Phys.* **5**, 944 (1964).

<sup>3</sup> M. E. Fisher, *Natl. Bur. Std. (U.S.) Misc. Publ.* **273**, 21 (1966); **273**, 108 (1966).

<sup>4</sup> M. J. Cooper and R. Nathans, *J. Appl. Phys.* **37**, 1041 (1966).

<sup>5</sup> B. E. Keen, D. P. Landau, and W. P. Wolf, *J. Appl. Phys.* **38**, 967 (1967).

<sup>6</sup> M. E. Fisher, *J. Appl. Phys.* **38**, 981 (1967).

<sup>7</sup> L. P. Kadanoff, D. Aspnes, W. Götze, D. Hamblen, R. Hecht, J. Kane, E. A. S. Lewis, V. Palciauskas, M. Rayl, and J. Swift, *Rev. Mod. Phys.* **39**, 395 (1967).

where  $A_{\pm}$ ,  $B_{\pm}$ ,  $\alpha$ , and  $\alpha'$  are constants,  $\epsilon \equiv (T - T_c)/T_c$ , and the subscripts  $\pm$  refer to  $\epsilon \gtrless 0$ . In the case of  $\alpha$  (or  $\alpha'$ ) equal to zero, Eq. (1) reduces to  $C \sim \ln \epsilon$ . Excluding size effects, Eqs. (1) are expected to be valid from the transition out to some relatively large  $\epsilon$  ( $\approx 10^{-1}$ ). Previous measurements<sup>8</sup> of the specific heat of manganese ammonium Tutton salt (MATS),  $\text{Mn}(\text{NH}_4)_2(\text{SO}_4)_2 \cdot 6\text{H}_2\text{O}$ , showed that a  $\lambda$ -type heat-capacity anomaly, a result of a magnetic ordering transition, existed at a temperature of about 0.173°K. Although measurements were carried only to within  $\pm 10^{-2} T_c$ , their qualitative features indicated that a rapid drop in heat capacity occurred within a temperature interval substantially less than  $\pm 10^{-2} T_c$ . This stimulated us to believe that perhaps MATS might be an ideal crystal for experimental study, so the present, more precise measurements were undertaken. MATS was also of interest to us since it is a material in which the interaction forces are relatively weak, as indicated by the small value of  $T_c$ . Further, the heat capacity is primarily due to magnetic interactions, the lattice contribution being negligible throughout the range of our measurements. Hence the difficulties common to high-temperature experiments in separating magnetic and lattice heat capacities are not present in this one. Moreover, the smaller the lattice heat capacity is with respect to the

<sup>8</sup> O. E. Vilches and J. C. Wheatley, *Phys. Rev.* **148**, 509 (1966).

magnetic heat capacity, the more readily details of the magnetic heat capacity may be resolved.

The principal experimental difficulties in studying a low-temperature transition are concerned with thermal equilibrium between sample and thermometer and with precise thermometry. Theoretical interpretation of the results may be difficult for a material with low  $T_c$  because the various types of magnetic interactions present may be of comparable size. Thus it would become difficult to sort out the effects of long-range and short-range forces in a low-temperature transition.

## II. EXPERIMENTAL METHOD

A detailed description has been published previously<sup>9</sup> of the apparatus and the general measuring technique, where sample, electric heater, and magnetic thermometer are submerged in liquid He<sup>4</sup> inside an epoxy resin cell. In Fig. 1 the general features of the heat-capacity cell are displayed. Details concerning the extraction of heat capacities from the measurements are given by Abel, Anderson, Black, and Wheatley.<sup>10</sup>

Thermal isolation from the rest of the cryostat is achieved by the use of an iron alum thermal guard between the cell and the He<sup>3</sup> refrigerator. Depending on its temperature, the guard makes possible measurements with very small negative, positive, or zero heat leaks in the range above 0.1°K, a feature which facilitates obtaining precise heat-capacity data with very small temperature jumps in this range. Thus, MATS is a material for which the present experimental approach can be used with great sensitivity.

The sample consisted of 10.53 g of small crystals (0.5–1.0 mm size) which seemed clear and of the right shape when examined under a microscope. The sample included those crystals used by Vilches and Wheatley in their experiment<sup>8</sup> and others from the same batch.

Experiments were made with two different thermometers. One consisted of 5.69 g of powdered cerium magnesium nitrate (CMN).<sup>11</sup> With this CMN mass about five times more sensitivity than in Ref. 8 was obtained in the heat-capacity measurements as a function of the absolute temperature. The other contained 4.96 g of small CrK alum (chrome alum) crystals. Another factor of 10 was added to the sensitivity,<sup>12</sup> but a way to convert the results from the chrome alum magnetic temperature scale to the absolute temperature had to be found. The conversion proved to be particularly simple, as described in the next section. The CMN thermometer was calibrated against the vapor pressure of He<sup>4</sup> with an error estimated conservatively to be no more than 1%. The chrome alum

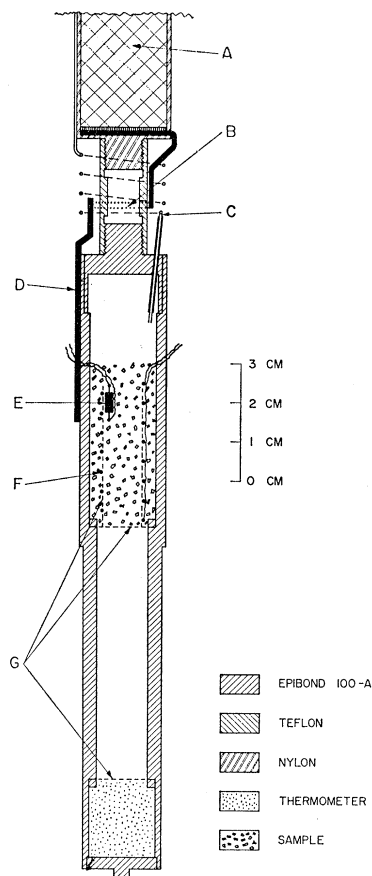


FIG. 1. Cell used for heat-capacity measurements with small sample crystals and liquid He<sup>4</sup>. (A) Iron alum thermal guard. (B) Lead switch. (C) Cupronickel He<sup>4</sup> filling tube. (D) Coil foil strip greased to cell. (E) Speer carbon resistor. (F) Heater. (G) Cotton cloth.

thermometer was also calibrated for convenience, and the "temperature" so defined called  $T^*$ .

The sensitivity of the 17-Hz mutual inductance bridge used for the temperature measurements was roughly one part in  $10^5$ . However, the precision with which temperature differences could be measured was determined primarily by long-term bridge stability. Temperature differences were determined with an accuracy of typically two or three microdegrees for the individual heat-capacity points. Long-term stability determined the precision with which  $\epsilon$  was measured.

Power was applied to the Evanohm heater for known periods of time in taking heat-capacity points. The total energy input from the heater was known to an accuracy better than 0.1%. Thus, the precision with which heat capacities were measured was determined only by the precision of the measurement of temperature differences. No data were obtained for  $|\epsilon| \gtrsim 3 \times 10^{-4}$  since the required size of the temperature jumps on putting in heat would have resulted in heat-capacity data of insufficient precision.

The correction to our heat-capacity data for the heat

<sup>9</sup> O. E. Vilches and J. C. Wheatley, *Rev. Sci. Instr.* **37**, 819 (1966).

<sup>10</sup> W. R. Abel, A. C. Anderson, W. C. Black, and J. C. Wheatley, *Physics (N.Y.)* **1**, 337 (1965).

<sup>11</sup> W. R. Abel, A. C. Anderson, and J. C. Wheatley, *Rev. Sci. Instr.* **35**, 444 (1964).

<sup>12</sup> D. de Klerk, *Handbuch der Physik*, edited by S. Flügge, (Springer-Verlag, Berlin, 1956), Vol. 15, p. 38.

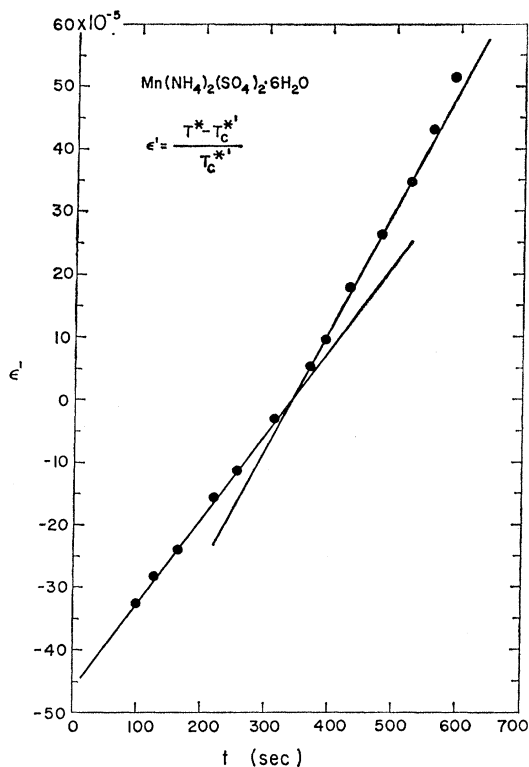


FIG. 2. A representative heating curve from which  $T_c$  was found. This curve was taken with the chrome alum thermometer.  $T^*$  is the uncalibrated magnetic temperature.  $\epsilon'$  is the parameter  $\epsilon' = (T^* - T_c^*)/T_c^*$  without correcting  $T_c^*$  for overshoot.

capacity of the  $\text{He}^4$  in the cell is less than 0.2% at our highest temperature point and is thus negligible for all of our data. As an additional precaution, dc residual magnetic fields at the sample were nulled to less than 0.05 G throughout the experiment.

### III. RESULTS

From an experimental point of view it has not always been possible to determine  $T_c$  with precision. Indeed, without some theory to unify the complex of experimental data on magnetic critical points, the meaning of  $T_c$  is frequently unclear and may be a question of semantics. In the present experiments, however, an empirical  $T_c$  could be defined and measured reproducibly to a precision in  $\epsilon$  of better than  $\pm 3 \times 10^{-5}$ . We therefore have not taken  $T_c$  to be a variable parameter in the present work. The method of defining  $T_c$  empirically is demonstrated in Fig. 2, which shows the variation of reduced temperature difference  $\epsilon'$  (defined in the caption to Fig. 2) with time when heat is applied at a constant rate. Assuming that the local slope of the curve is inversely proportional to the heat capacity, one sees that within a range of  $\epsilon'$  less than  $\pm 10^{-4}$  in width the heat capacity changes very rapidly. The temperature corresponding to the intersection of straight lines through the data points immediately

before and immediately afterward can be determined and reproduced to a precision in  $\epsilon$  of better than  $\pm 3 \times 10^{-5}$ , as previously mentioned. The temperature corresponding to this intersection, corrected by a known amount for overshoot, was taken as  $T_c^*$ . The heating curves obtained with the CMN thermometer are similar in shape to Fig. 2 with the  $\epsilon$  scale about ten times coarser. Since the reduced uncertainty in  $T_c^*$  is substantially smaller than the smallest  $\epsilon$  for any of our heat-capacity points, the effect of this uncertainty on the cross calibration of the CMN and chrome alum thermometers was negligible.

The value of  $T_c$  for MATS found in this experiment is about  $0.176^\circ\text{K}$ , subject to an error of less than 1% in calibrating the absolute temperature scale for the CMN thermometer. The difference between this value and that of  $0.173^\circ\text{K}$  quoted by Vilches and Wheatley is well within the combined calibration errors of the two experiments. For each experimental run we used the value (or values) of  $T_c$  determined in it to calculate  $\epsilon$ . However, the absolute values of  $T_c$  for the four runs with the chrome alum thermometer were all within  $\pm 6 \times 10^{-6}^\circ\text{K}$  of the average, corresponding to  $\pm 3 \times 10^{-5}$  in  $\epsilon$ .

Additional qualitative information about the nature of the transition was obtained by analysis of the data on Fig. 2 and of similar data from other runs using the chrome alum thermometer. Table I presents both the ratios of the slopes of the heating curves immediately above and below  $T_c$  and the corresponding changes in  $C/nR$ , where  $n$  is the number of moles and  $R$  is the gas constant, determined using these and heating-rate data. Examination of the table and of Fig. 2 shows that within a range of  $\epsilon$  of about  $\pm 10^{-4}$  of the transition the molar heat capacity changes by about  $R$ .

Using the CMN thermometer the data were of insufficient precision for  $|\epsilon| \lesssim 10^{-3}$ . With the more sensitive chrome alum thermometer it was possible to obtain sufficiently precise data for  $|\epsilon| \gtrsim 3 \times 10^{-4}$ . In the case of the CMN thermometer, for which the heat capacity is negligible in this range compared with that of MATS, the heat capacity is determined directly in terms of  $\epsilon$ . In the case of the chrome alum thermometer, however, a total cell heat capacity  $C^*$  is obtained which is a combined heat capacity of the MATS sample

TABLE I. Transition-point data.

Run	$\dot{Q}$ (ergs/sec)	$\Delta(C/nR)^a$	Slope ratio <sup>a</sup>
CrK alum-1	3.02	1.4	1.5
CrK alum-2	1.08	0.3	1.1
CrK alum-3a <sup>b</sup>	2.27	1.3	1.5
CrK alum-3b <sup>b</sup>	0.99	0.7	1.2
CrK alum-4	1.30	1.0	1.3

<sup>a</sup> Corrected for the heat capacity of the chrome alum.

<sup>b</sup> Heat leak was negative here, allowing us to go through the transition twice in the same run.

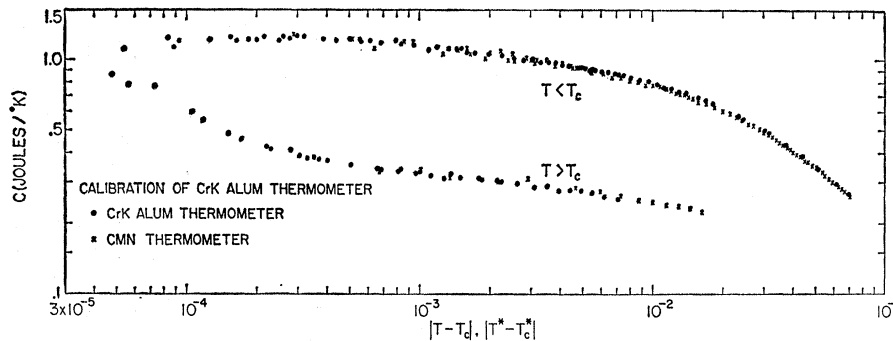


FIG. 3. Calibration of the chrome alum thermometer.  $C^*$  versus  $T^* - T_c^*$  and  $C$  versus  $T - T_c$ .  $C$  is adjusted to include the heat capacity of the chrome alum in the thermometer.

and the chrome alum, based on the magnetic temperature indicated by the chrome alum. The critical point of MATS occurs at a well-defined temperature  $T_c^*$  on the chrome alum scale. In Fig. 3 we have plotted the total heat capacity  $C^*$  against  $T^* - T_c^*$ . On the same figure we have plotted against  $T - T_c$  a heat capacity  $C$ , which is the sum of the heat capacities of the same MATS sample and of the chrome alum thermometer<sup>3</sup> as determined by CMN thermometry. Inspection of this figure shows that out to values of  $|T - T_c|$  or  $|T^* - T_c^*|$ , well beyond where the two types of data overlap, there is no significant difference between  $C$  and  $C^*$ . It follows that, for values of  $|T - T_c|$  or  $|T^* - T_c^*|$  less than at least  $7 \times 10^{-3}$  °K, one has with sufficient accuracy

$$T^* - T_c^* = T - T_c. \quad (2)$$

For values of  $T^* - T_c^*$  less than  $7 \times 10^{-3}$  °K we there-

fore obtained the heat capacity of MATS by subtracting from the total heat capacity that of the chrome alum thermometer using smoothed data of Vilches and Wheatley.<sup>8</sup> The quantity  $\epsilon$  for each point was obtained, following Eq. (2), by dividing  $T^* - T_c^*$  by  $T_c$ . Data obtained with the chrome alum thermometer, so corrected, together with data obtained with the CMN thermometer, are listed in the Appendix for values of  $|\epsilon| < 2 \times 10^{-2}$ .

Corrected data using the chrome alum thermometer, together with data using the CMN thermometer, are displayed in Fig. 4 on (a) semilogarithmic and (b) full logarithmic plots of  $C/nR$  versus  $\epsilon$ . The triangles of Fig. 4 (a) are the data of Vilches and Wheatley. Some of our data have been omitted for clarity in the figure. The heat capacity can be fitted by either a simple logarithmic law or a power law over about  $1\frac{1}{2}$  decades in  $\epsilon$  below  $T_c$  and two decades above  $T_c$

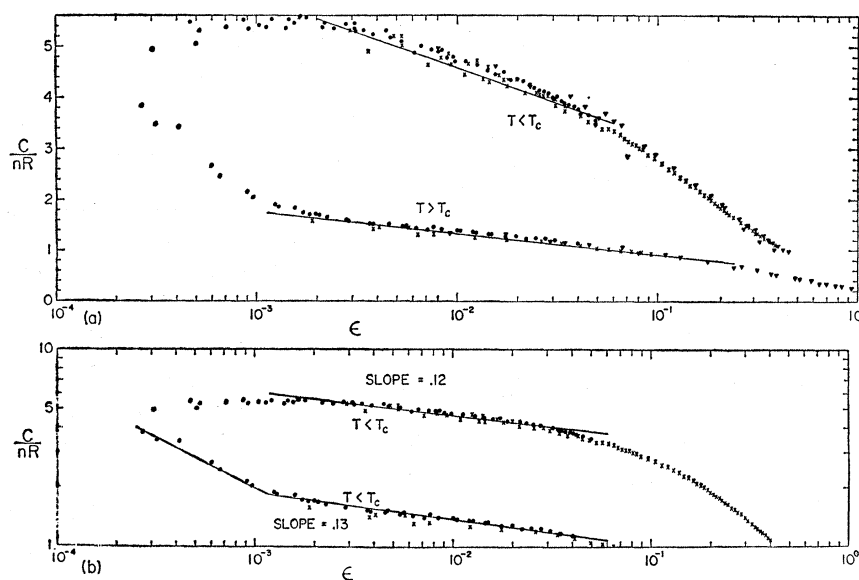


FIG. 4. Heat capacity of  $\text{Mn}(\text{NH}_4)_2(\text{SO}_4)_2 \cdot 6\text{H}_2\text{O}$  plotted on (a) semilog and (b) full logarithmic scales. The solid lines show the range of logarithmic- and power-law fits to the data.  $\times$  CMN data.  $\circ$  Chrome alum data.  $\nabla$  Vilches and Wheatley data.

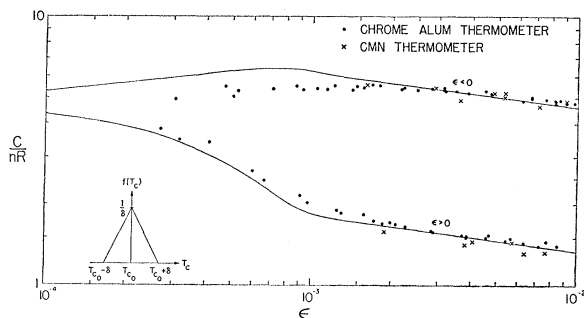


FIG. 5. Heat capacity of  $\text{Mn}(\text{NH}_4)_2(\text{SO}_4)_2 \cdot 6\text{H}_2\text{O}$  plotted on a full logarithmic scale. The solid curves are calculated values based on a simple model in which the measured heat capacity is assumed to be a super position of "ideal" heat-capacity curves with a distribution of critical temperatures  $T_c$ . The inset at lower left shows the assumed triangular distribution function for  $T_c$  used to calculate the solid curves.

for  $|\epsilon| \lesssim 10^{-3}$ . Below  $T_c$ , a rounding effect is observed for  $|\epsilon| < 10^{-3}$ ; above  $T_c$ , a rather rapid decrease of the heat capacity is observed for  $\epsilon < 10^{-3}$ . The equations of the power-law fits to the data for  $|\epsilon| > 10^{-3}$  are

$$\begin{aligned} C_+/R &= 2.55\epsilon^{-1/8}, & 10^{-3} \leq \epsilon \leq 4 \times 10^{-2} \\ C_-/R &= 0.75|\epsilon|^{-1/8}, & 2 \times 10^{-3} \leq |\epsilon| \leq 3 \times 10^{-2}. \end{aligned} \quad (3)$$

#### IV. DISCUSSION

Theoretical predictions of  $\alpha$  and  $\alpha'$  have been made on the basis of the three-dimensional Ising model. It had been expected that  $0 \lesssim \alpha \lesssim 0.2$  and  $0 \lesssim \alpha' \lesssim 0.06$ .<sup>1,7</sup> Domb<sup>13</sup> has suggested recently that  $\alpha \simeq \alpha' \simeq \frac{1}{8}$ . Excluding size effects Eqs. (1) are expected to be valid from the transition out to some relatively large  $\epsilon$  ( $\approx 10^{-1}$ ).

We find in our experiment that  $\alpha \simeq \alpha' \simeq \frac{1}{8}$  for MATS, but only over a limited range of  $\epsilon$ . For  $|\epsilon| < 10^{-3}$ , the heat capacity is no longer described by the  $\epsilon^{-1/8}$  laws, and there is a pronounced rounding of the heat capacity below  $T_c$ . Similar behavior has been observed for the transitions in  $\text{CoCl}_2 \cdot 6\text{H}_2\text{O}$ <sup>14</sup> ( $T_c = 2.29^\circ\text{K}$ ),  $\text{RbMnF}_3$ <sup>15</sup> ( $T_c = 83.0^\circ\text{K}$ ),  $\text{EuO}$ <sup>16</sup> ( $T_c = 69^\circ\text{K}$ ), and  $\text{Gd}$ <sup>17</sup> ( $T_c \simeq 290^\circ\text{K}$ ) at roughly the same values of  $|\epsilon|$ . Hence the "rounding" phenomenon is probably not correlated with the magnitude of  $T_c$ . In fact, the only magnetic transition known to us for which heat-capacity data exist for  $|\epsilon| < 10^{-3}$  and for which this "rounding" effect has not been observed is  $\text{MnF}_2$ <sup>18</sup> ( $T_c = 67.33^\circ\text{K}$ ).

It is therefore important to consider possible sources

for the departures of the heat capacity from the  $\epsilon^{-1/8}$  laws for values of  $|\epsilon| < 10^{-3}$ . In the present experiment these departures may be described qualitatively as follows. Approaching  $T_c$  (as defined in this paper) from below, the heat capacity increases approximately as  $|\epsilon|^{-1/8}$  until  $|\epsilon| \approx 10^{-3}$ . For smaller values of  $|\epsilon|$ , the heat capacity has a broad maximum and decreases slightly before reaching the transition. Within  $|\epsilon| \approx \pm 10^{-4}$  of the "transition," the molar heat capacity decreases by about  $R$  as temperature increases. There is then a relatively rapid decrease of heat capacity with increasing temperature until  $\epsilon \approx 10^{-3}$ . For larger values of  $\epsilon$  the heat capacity varies as  $\epsilon^{-1/8}$ .

Our sample consisted of hundreds of small crystals. It is conceivable that  $T_c$  is not the same for all the crystals in the sample or that even within the same crystal  $T_c$  could vary from point to point. We have therefore made a simple analysis in which we assume that the heat capacity of an ideal crystal is given by Eqs. (3), but in which there is a distribution of  $T_c$  about some value  $T_{c0}$ . In Fig. 5 we show the results of a calculation using a triangular distribution function symmetrical about a temperature  $T_{c0}$  and with contributions out to  $\delta = 10^{-3}T_{c0}$ . The calculated heat capacities are plotted against  $\epsilon \equiv (T - T_{c0})/T_{c0}$ . Although there is not excellent agreement between the calculated curve and experimental points, the general features of the departures from the  $\epsilon^{-1/8}$  power laws are indeed evident. These are a broad maximum for  $T < T_{c0}$ , a relatively rapid drop just above  $T_{c0}$ , and a change of molar heat capacity of about  $R$  for values of  $|\epsilon| < 10^{-4}$ . Hence it seems likely that the general features of the heat-capacity data for  $|\epsilon| < 10^{-3}$  could be explained by an ideal behavior given by Eqs. (3) and an appropriate distribution function for  $T_c$ , though we have not attempted to find a quantitatively correct distribution function based on the data.

We do not know the source of the distribution in  $T_c$  which must be postulated to explain the data for  $|\epsilon| < 10^{-3}$  while maintaining an  $\epsilon^{-1/8}$  law to describe an ideal critical behavior of MATS. Domb<sup>13</sup> has calculated the rounding of the transition due to the finite size of the crystals. For crystals of the size present in our sample, departures due to size effects should not occur for  $|\epsilon| > 10^{-5}$ . Hence size effects should not be responsible for the present results.

#### ACKNOWLEDGMENTS

We are grateful to Professor C. P. Slichter and Professor L. P. Kadanoff, and to R. Hecht for helpful discussions concerning the interpretation of our experimental results.

#### APPENDIX

Table II presents corrected data on the specific heat of MATS as a function of  $\epsilon$  as obtained using the cerium-magnesium-nitrate and chromium-potassium-alum thermometers.

<sup>13</sup> C. Domb, Ann. Acad. Sci. Fennicae AVI, 167 (1966).

<sup>14</sup> J. Skalyo, Jr., and S. A. Friedberg, Phys. Rev. Letters 13, 133 (1964).

<sup>15</sup> D. T. Teaney, V. L. Moruzzi, and B. E. Argyle, J. Appl. Phys. 37, 1122 (1966).

<sup>16</sup> D. T. Teaney, Ref. 5, p. 50.

<sup>17</sup> A. V. Voronel', S. R. Garber, A. P. Simkina, and I. A. Charkina, Zh. Eksperim. i Teor. Fiz. 49, 429 (1965) [English transl.: Soviet Phys.—JETP 22, 301 (1966)].

<sup>18</sup> D. T. Teaney, Phys. Rev. Letters 14, 898 (1965).

TABLE II. Corrected data for  $|\epsilon| < 2 \times 10^{-2}$ .

A. CMN data		$\epsilon \times 10^3$	$C/nR$	B. CrK alum data		$\epsilon \times 10^3$	$C/nR$
$\epsilon \times 10^3$	$C/nR$			$\epsilon \times 10^3$	$C/nR$		
17.8	4.22	18.8	4.34	2.49	5.35	4.57	1.50
13.6	4.36	17.3	4.50	2.17	5.37	5.43	1.47
9.36	4.65	15.9	4.44	1.80	5.56	6.33	1.44
4.85	5.20	14.4	4.52	1.57	5.45	7.21	1.40
17.1	4.35	12.8	4.63	1.22	5.52	8.47	1.40
14.2	4.59	11.2	4.70	0.875	5.52	10.5	1.38
11.3	4.66	9.68	4.78	0.526	5.30	12.2	1.36
8.32	4.77	8.19	4.89	0.271	3.83	14.6	1.32
5.33	5.01	6.70	5.02	0.602	2.66		
2.92	5.31	4.73	5.17	0.911	2.15		
1.89	1.58	3.14	5.44	1.26	1.89		
4.08	1.45	1.48	5.52	1.59	1.83		
6.37	1.31	1.87	1.70	2.00	1.71		
19.8	4.36	3.86	1.51	2.28	1.65		
18.1	4.35	9.91	4.69	2.84	1.60		
16.3	4.44	9.05	4.77	3.86	1.51		
14.5	4.31	8.56	4.92	4.68	1.53		
12.6	4.71	7.57	4.93	5.67	1.49		
10.9	4.46	6.70	4.97	7.70	1.46		
9.06	4.85	6.20	4.87	10.1	1.40		
7.16	4.64	5.38	5.09	12.7	1.36		
5.32	5.19	4.49	5.30	15.0	1.32		
3.62	4.90	3.88	5.22	17.6	1.28		
1.63	5.57	3.13	5.34	1.42	5.35		
3.82	1.42	2.21	5.46	1.04	5.42		
5.75	1.44	1.68	5.58	0.924	5.34		
7.65	1.32	1.14	5.37	0.473	5.48		
12.3	1.27	0.715	5.37	0.319	3.47		
17.7	1.23	0.508	5.05	0.666	2.45		
		0.307	4.94	0.971	2.04		
		0.414	3.41	1.30	1.85		
		3.48	5.31	1.73	1.73		
		3.18	5.28	2.08	1.68		
		2.83	5.43	2.91	1.57		
				3.71	1.53		